

Monochromator used to select x-rays for diffraction experiments with nanosecond time-resolution. A white x-ray beam enters from the left and strikes a triangularly-cut single-crystal monochromator. The horizontal wheel at the apex of the triangular crystal (just left of the center of the photograph) is actually a motor-driven cam that bends the monochromator crystal to focus horizontally the diffracted x-ray beam at the sample. The long device to the right of the monochromator is a float glass mirror used in a total external reflection arrangement to remove higher-harmonic wavelengths from the diffracted beam.

Synchrotron Radiation Research: Number 2

# Time-resolution experiments using x-ray synchrotron radiation

Scientists in fields ranging from condensed-matter physics to biochemistry are taking advantage of the natural temporal structure of the high-intensity x rays emitted by sources of synchrotron radiation.

Dennis M. Mills

Many important biological, chemical and physical phenomena take place on time scales of nanoseconds or picoseconds. Those working to unravel the time development of such fast processes have long recognized that pulsed electromagnetic radiation and particle beams often make more incisive probes than do continuous emissions. During the last decade, a powerful new device joined the arsenal of modulated radiation sources available to scientists attacking problems that require good temporal resolution—the high-energy storage ring.

Users of visible and ultraviolet synchrotron radiation were the first to take advantage of the pulsed nature of storage-ring emissions, and there are several excellent articles' that survey their work. My purpose in this article is to discuss recent time-resolution studies that use storage-ring emissions in the x-ray region of the spectrum,

Dennis Mills is a staff scientist at CHESS, the Cornell High-Energy Synchrotron Source, in Ithaca, New York.

above energies of 3000 eV. Investigators are making use of this radiation to study the temporal development of a wide variety of dynamic phenomena, including, for example,

- ▶ nuclear resonant, or "Mössbauer," fluorescence
- ▶ ultrafast (10 m/sec) defect-free recrystallization of silicon
- ▶ interaction of megahertz acoustic waves with dislocations in crystals
- ▶ electronic rearrangement in an atom following the creation of an innershell vacancy.

On the horizon are applications to biological problems such as the molecular dynamics of proteins, an example that I will discuss later in some detail.

Considering that storage rings have been used as a source of x-rays for nearly ten years, it is not altogether clear why it is only in the last several years that experimenters have seriously considered using this portion of the synchrotron radiation spectrum for time-resolution investigations. Nonetheless, the number of people using storage-ring sources for x-ray experi-

ments that emphasize time resolution is growing rapidly as awareness of the

intriguing possibilities spreads. To best appreciate the gains that storage-ring sources may bring to x-ray studies that require good time resolution, it is useful to compare the temporal and spectral properties of x-ray synchrotron radiation with a representative sampling of radiation from other pulsed x-ray sources. Table 1 makes such a comparison. Three points deserve attention. First, the spectra from these other sources often contain a mix of both Bremsstrahlung and characteristic lines, in contrast with the smoothly varying spectrum from storage rings. Second, only the x-ray pulses from laser-generated plasmas have durations as short as those in synchrotron radiation bursts. And third, only synchrotron radiation sources operate at very high repetition rates. It is interesting that the radiation emitted from storage-ring sources, with its high repetition rate, short pulse duration and continuous spectrum, is very reminiscent of the radiation of the modelocked dye laser, which has produced such a wealth of information in optical studies of transient phenomena.

## Temporal structure

The pulsed nature of the radiation emitted from storage rings arises from the fact that the accelerated particlesthe stored electrons or positrons-are not distributed continuously around the circumference of the ring, but are grouped in packets or bunches by the ring's radiofrequency cavities that replenish their energy.2 Storage rings are constructed such that the rf accelerating frequency is some multiple of the rotational frequency of the particles. This multiple becomes the number of equally spaced stable orbit positions, or rf "buckets," in which particles can be stored. The time between radiation bursts that an experimenter observes is a function of the number and configuration of filled rf buckets. The maximum time between bursts occurs in the "single-bunch mode," in which only one bunch of particles is in the ring, and the minimum time between bursts occurs in the "multi-bunch mode," in which all the buckets are filled. Interpulse periods can range from a few nanoseconds to a few microseconds for large accelerators running in a single-bunch mode. (See table 2.) The interpulse period of a particular storage ring often depends on whether the ring is being run as a dedicated source for synchrotron radiation or is being used for high-energy physics.

Typical bunch lengths vary from hundreds of picoseconds to several nanoseconds. Table 2 lists both the interpulse periods and bunch durations for x-ray storage rings around the world. It is important to note that the temporal properties described above hold for all emitted wavelengths of radiation, that is, the emitted pulse shapes and widths are independent of wavelength<sup>3</sup>

There are several beam parameters that are particularly important for attaining good experimental temporal resolution: temporal "purity," the magnitude and stability of the interpulse period, and the magnitude and stability of the bunch length.

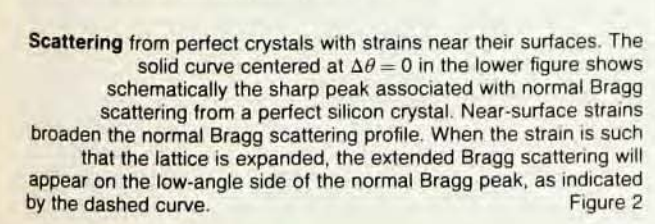
▶ Temporal "purity" is a measure of the degree to which rf buckets intended to remain unfilled have indeed remained empty during the filling of the targeted buckets. Partially filled satellite bunches are of no consequence if eventually all the buckets in the ring are to be filled, but can be detrimental to those timing experiments that require a single well-defined pulse with no other radiation in the intervening periods.

- ▶ The interpulse period is probably one of the better-known temporal parameters of a storage ring. Absolute measurements in typical storage-ring time regimes are relatively easy to make. The stability of the revolution frequency is determined by the stability of the clock driving the rf accelerating system. The precision of the quartz oscillator clocks used is typically one part in 10<sup>7</sup> to 10<sup>8</sup>, corresponding to a jitter of the orbital period of less than 10<sup>-2</sup> picoseconds.
- ▶ Bunch shape characteristics are more difficult to measure because of the shorter time scales involved. A model assuming no interactions within a particle bunch in a storage ring predicts a Gaussian distribution for the particle density in the bunch. Several research groups at various storage rings have verified this prediction at low beam currents by measuring average bunch profiles. At very short bunch lengths and high particle densities, however, this model is no longer valid. Investigators doing a machine physics study at the Stanford Synchrotron Radiation Laboratory observed bunch modulations of both low and high frequency. Using an x-ray streak camera-the only apparatus available with the requisite sensitivity and temporal resolution-they saw modulations of under 10 kHz and also of 10 to 50 GHz.

#### Time-resolution experimentation

In the discussion that follows, I focus on experiments that take direct advantage of the pulsed nature of the x rays, can be cyclically pumped or probed, and have time scales of interest of much less than a millisecond when using the x rays as a probe, or require a short excitation pulse when the x rays are used as a pump. Of course, one can carry out investigations of phenomena that occur on a time scale longer than a millisecond; however, such experiments generally do not take advantage of the time structure of the emitted radiation but rather rely on the extremely high flux from storage-ring sources to decrease data-collection time.

In 1978, Richard Cohen and his coworkers at Bell Laboratories reported the first explicit use of the time structure of the x rays emitted from a storage-ring source, in a study of nuclear resonant, or Mössbauer, fluorescence.4 In normal Mössbauer spectroscopy, a radioactive parent makes a nuclear transition to the ground state, emitting a gamma ray of extremely well-defined energy ( $\Delta E/E$  ranges from  $10^{-9}$  to  $10^{-13}$ ), which can be reabsorbed by a similar nucleus. Due to the sharpness of the fluorescent line, small changes in the energy levels of an absorbing nucleus can shift the resonant energy level significantly, so that the emitted gamma ray may no longer be resonantly absorbed. This extreme sensitivity to energy levels affords a valuable probe of the local environment of the absorbing nucleus. Unfortunately, this eloquent and powerful tool can only be used on nuclei with naturally occuring radioactive parents. By using the high spectral brightness of the synchrotron radiation to excite potential Mössbauer states for which there are no naturally occuring radioactive parents, one may hope to open up a completely new class of materials to Mössbauer spectroscopy. The Bell Labs group used the pulsed nature of



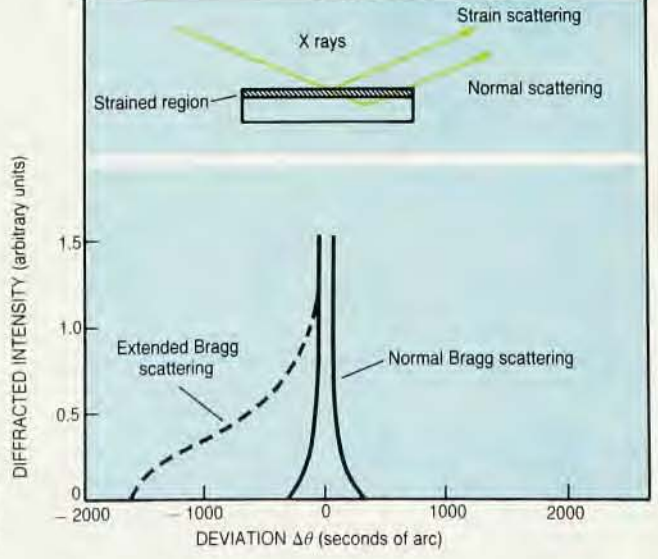


Table 1. Pulsed x-ray sources

Source of x rays	Pulse length	Repetition rate	Spectral properties	
Pulsed x-ray generators	10 to 100 nsec	1 to 100 Hz	Characteristic x-ray lines from anode in the 5-20 keV range; some bremsstrahlung	
Pulsed electron linear accelerators	10 to 100 nsec	0.1 to 100 Hz	Mostly bremsstrahlung (can be very hard)	
Laser-produced plasmas	0.1 to 10 nsec (same duration as laser pulse)	0.0001 to 0.01 Hz	Bremsstrahlung and some discrete line in the 0.5-5 keV range	
Synchrotron radiation sources	0.05 to 2 nsec.	0.4 to 50 Mhz	Continuous spectrum from infrared to hard x rays	

the exciting x-ray beam to decrease the background of non-nuclear fluorescence, which is the predominant experimental problem in nearly all work in artificially excited Mössbauer states. Although this pioneering experiment did not attempt to use the scattered nuclear resonant radiation, it stimulated more ambitious studies not only in the area of nuclear resonant fluorescence but in the general area of x-ray studies that emphasize time resolution.

Nanosecond-resolution diffraction. One of the first x-ray diffraction experiments to utilize the temporal structure of synchrotron radiation was an investigation-on a nanosecond time-scaleof melting and recrystallization phenomena in silicon during pulsed laser annealing. It has been known for several years that lattice damage within a micron of the silicon surface is completely removed upon illumination with high-power pulsed laser radiation (1 J/cm2, 15 nsec fwhm). Surface reflectivity measurements with good time resolution indicate that under these conditions the annealing process lasts only 100 nsec. Considering the depth of the annealed layer, this corresponds to a seemingly phenomenal defect-free regrowth rate of 10 m/sec! Normal silicon crystal growth rates are several mm/min or about 10-4 m/sec. The ultra-rapid melting and recrystallization rates stimulated researchers to look in more detail at the energy transfer mechanisms associated with pulsed laser annealing, and from these studies two different thoughts have developed.

One picture of the annealing process is simply that it is a classical thermal melting phenomenon,<sup>5</sup> that is, the energy from the laser, initially absorbed by the electrons, is rapidly transferred to the crystal lattice, causing the damaged near-surface region to melt. This melted layer then regrows epitaxially from the unmelted, undamaged region as the heat flows into the bulk silicon. The thermal model implies that the lattice temperature at the liquid-solid interface is at or near silicon's classical melting temperature of 1410 °C

An alternative to this description is the plasma model, in which the electrons that absorb the laser energy retain it for a much longer time than they do in the thermal model. This causes the silicon to go "gently" into a fluid state through a loss of shear resistance that comes about due to the large fraction of electrons that have been excited out of bonding states.6 These softened bonds allow the atoms to arrange themselves in their lowestfree-energy configuration—the crystalline state. In the plasma model, the lattice temperature need not reach the classical melting temperature to account for the observed annealing, and in fact the temperature is predicted to reach only a few hundred degrees centrigrade during annealing. Several experimenters have attempted to measure the near-surface lattice temperature of silicon during annealing, but their differing results have been unable to resolve the controversy.

Recently, however, Bennet Larson and his colleagues at Oak Ridge National Laboratory devised x-ray diffraction techniques with nanosecond resolution and measured both the temperature and temperature gradients in silicon during pulsed laser annealing.7 In these experiments, carried out with my collaboration at the Cornell High-Energy Synchrotron Source, we monitored the temperature indirectly by looking at the temporal behavior of thermally generated strains near the surface of silicon. We did this by synchronizing the firing of a 15-nanosecond ruby-laser pulse and the 160picosecond burst of x rays emitted from CHESS. Figure 2 shows a well-known technique for determining the profiles of static strain near the surface of a crystalline material by measuring the extended Bragg scattering profile in the vicinity of the normal Bragg peak. We have expanded this method to dynamic studies by measuring the extended Bragg scattering at various times after the arrival of the annealing laser pulse.

Bragg reflections from perfect single crystals occur over a very small angular range, typically tens of arc seconds. However, if the crystal has lattice strains, then the width of the Bragg reflection is broader according to the differentiated form of Bragg's law

$$\Delta d/d = -\cot\theta_{\rm h} \Delta\theta$$

Here  $\Delta d/d$  is the strain,  $\theta_b$  the nominal Bragg angle and  $\Delta\theta$  the angular width of the extended Bragg reflection. With a more detailed analysis, one can calculate not only the breadth  $\Delta\theta$  of the extended Bragg scattering for a given strain profile  $\Delta d/d$ , but also the magnitude of the scattering intensity as a function of angle. By inverting this procedure, one can infer the strain profile in a crystal from the shape of the extended Bragg profile. Assuming that the extended Bragg scattering is due only to the strains, that is, ruling out dislocations or grain boundaries that could contribute to line broadening, and assuming the strains are thermal in nature, then with the use of temperature-dependent thermal expansion coefficients, it is a straightforward procedure to transform the strain profiles into thermal profiles.

Figure 3a shows the extended Bragg scattering profiles near the Si(111) reflection at 20, 55 and 155 nanoseconds after a 1.5 joule/cm2 ruby laser pulse impinged on the sample. Data taken on the positive- $\Delta\theta$  side of the Bragg reflection show that the peak is not simply broadened (which would be the signature of crystal defects within the lattice) but is only extended toward the one side, indicating a lattice expansion. Figure 3b shows the corresponding time-resolved thermal profiles obtained from the extended Bragg scattering profiles of figure 3a. The salient feature of the data in figure 3b is that the 20- and 55-nsec curves at the solid-liquid interface reach the classical melting temperature of silicon, strongly supporting the thermal melting model.

We are continuing these studies to include other semiconductor materials, and we will be looking more closely at superheating and undercooling effects during the ultrarapid melting and cry-

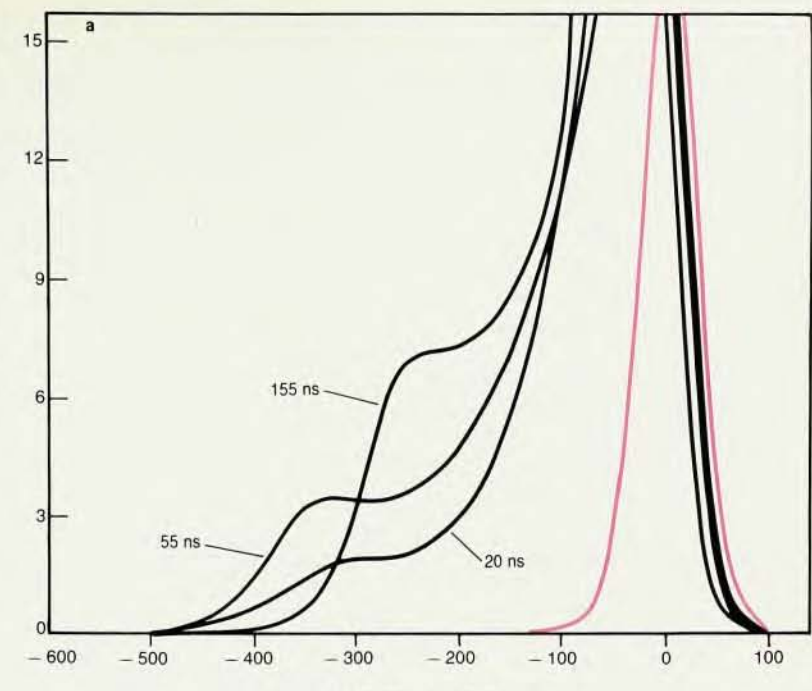
stallization processes. Stroboscopic topography. One commonly-used technique for characterizing crystal defects is x-ray topography, in which one makes two-dimensional images of lattice strains. Two independent groups recently used this technique stroboscopically to make the first time-resolution studies of the interaction of acoustic waves and crystal defects. Figure 4 shows a typical experimental geometry for x-ray topographic studies. White synchrotron radiation strikes the sample (depicted here in the Bragg or reflection geometry) and the diffracted images are recorded on a photographic plate. Changes in the reflectivity of the sample produce contrast on the film. Slowly varying strains cause no contrast. However, when lattice strains vary over short distances, that is, distances within an x-ray extinction depth, the local reflectivity can increase. By synchronizing acoustic vibrations in crystals with the fundamental or a harmonic multiple of the repetition rate of the emitted x-rays, one can produce a "time-frozen" or stroboscopic picture of the strain fields.

At the Hamburg Synchrotron Radiation Laboratory at DESY, Claus-Christian Glüer of the University of Hamburg and his collaborators have used this technique to study the dynamic interactions of dislocations with bulk acoustic waves in quartz. By driving a crystal at the 1.04 Mhz frequency of the synchrotron radiation pulses, the Hamburg group detected motion and contrast changes of dislocations on a timescale as short as 4 nanoseconds—the first direct imaging of dislocation motion due to ultrasonic

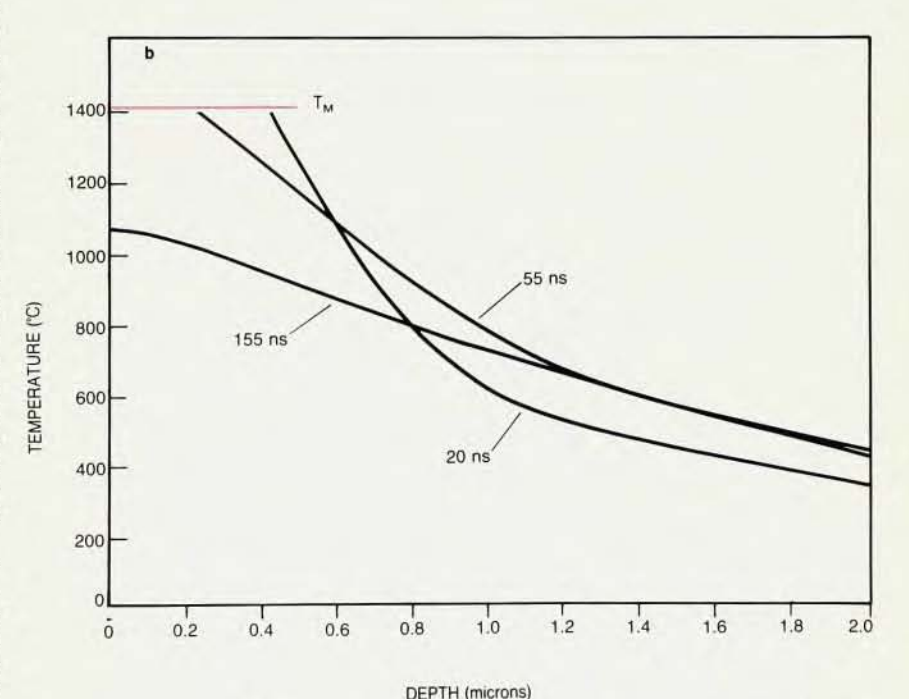
P. A. Goddard of Durham University and his colleagues working at the Synchrotron Radiation Source in Daresbury, England, used this method to image traveling Rayleigh waves in LiNbO<sub>3</sub> surface-acoustic-wave (SAW) devices.9 In one experiment, the excited SAW device, a 38-Mhz LiNbO3 intermediate frequency television filter, was phase locked to the 12th harmonic of the 3.122 Mhz pulse frequency of the x rays emitted from the Daresbury storage ring. Figure 5 is a stroboscopic image from the experiment. The periodic dark and light bands are strains in the crystal; the thick jogged white line is a grain boundary. From an image such as this, one can determine both the amplitude and the phase of the traveling surface acoustic wave. Besides providing an ideal diagnostic tool for SAW-device technology, stroboscopic topography is sure to produce a wealth of information on the interaction between acoustic waves and crystal defects.

Absorption spectroscopy. Our understanding of proteins has advanced enormously over the last 25 years through the use of a wide variety of techniques that reveal the time averaged or static three-dimensional structure of these large molecules. Over the last several years, however, an increasing number of scientists have come to believe that static models of proteins cannot explain many of the complex properties that are observed experimentally. As a result, dynamic pictures of proteins are beginning to emerge that indicate that dynamic features to a large extent control many of the biological functions of proteins. 10

To date, nearly all time-resolution studies of dynamic processes in pro-

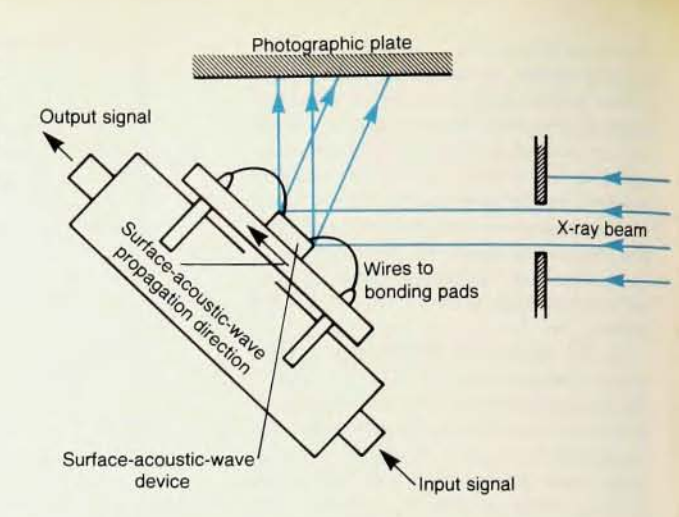


DEVIATION  $\Delta\theta$  (seconds of arc)



Extended Bragg scattering in silicon resolved in time during pulsed laser annealing. Part a shows the extended Bragg scattering profiles near the Si(111) reflection for three different times after the arrival of the laser pulse. The colored line represents the "no-laser" profile. At the two shorter times (20 and 55 nsec), the Bragg scattered intensity reaches to — 500 arc sec while the 155 nsec profile extends to less than — 400 arc sec, indicating a more dilated (higher-temperature) lattice at shorter times. Part b shows the lattice temperature profiles corresponding to the extended Bragg scattering measurements. The 20 and 55 nsec curves show a maximum temperature very near the melting point of silicon, 1410 °C.

Stroboscopic topography experimental geometry. The incident white beam is collimated and allowed to strike the sample, in this case, a surface-acoustic-wave device. Topographs are recorded on nuclear emulsion film approximately 2.5 cm from the Figure 4 sample.



teins have involved transient optical methods. In collaboration with Aaron Lewis at Cornell University, our research group at CHESS has begun to investigate the feasibility of using x-ray spectroscopic time-resolution techniques to study molecular dynamics and cooperativity in biological systems.

One of the problems we are investigating is the kinetics of ligand binding in proteins. We do this by studying the recombination of the carbon monoxide ligand with the iron atom in myoglobin (Mb) after laser flash photodissociation.

Myoglobin, the protein in muscles that stores oxygen until it is required for metabolic oxidation, has a single, internally located iron atom that is octahedrally coordinated in the ligated state. Much like hemoglobin, which carries oxygen in the blood, myoglobin is "poisoned" by carbon monoxide because the CO molecule dissociates less easily than does the O2 molecule. As knowledge of the three-dimensional structure of myoglobin became more refined, it became apparent that there is no clear channel for the CO ligand to enter the protein from outside and proceed to the iron site. This led to the realization that the important physiological process of ligand binding requires that a major structural reorganization occur, and hence must depend strongly on fluctuations or transient alterations in the protein structure. Detailed laser studies of the transient phenomenon of ligand photolysis and recombination have revealed that this is in fact the case, and that during ligation myoglobin undergoes both electronic and structural alterations

Table 2. X-ray storage rings

Facility	Stored beam energy (GeV)*	Critical photon energy (keV)*	Orbital period (nsec)	Number of equally spaced bunches	Interpulse period (nsec)	Bunch duration fwhm (psec)
ADONE Frascati, Italy	1.5	1.5	350	3 18 1	117 19.4 350	776
LURE (DCI) Orsay, France	1.7	3.1	316	1	316	1780
SRS Daresbury, UK	2.0	3.9	320	160	2	200
Photon factory Tsubuka, Japan	2.5	4.0	624	312	2	160
NSLS (x ray) Brookhaven, New York	2.5	5.0	568	30	18.9	1700
SSRL (SPEAR) Stanford, California	3 (4)	4.7 (11.1)	760	4×4ª 4 <sup>b</sup> 1°	187×2.8 <sup>a</sup> 190 760	300
HASYLAB (DORIS) Hamburg, W. Germany	3.7 (5)	7.8 (22.9)	960	60 170 1 <sup>c</sup>	16 8 960	200
VEPP-4 Novosibirsk, USSR	4.5 (5.8)	12.2 (26.1)	1220	t	1220	400
CHESS (CESR) Ithaca, New York	5 (8)	8.7 (35.5)	2560	1 3 7 <sup>d</sup>	2560 853 366	160

<sup>\*</sup>Parenthetical numbers indicate maximum design parameters.

\*Four equally spaced groups of four adjacent bunches.

SSRL periodically runs in a timing mode with four equally spaced bunches.

Parasitic running conditions.

that span the picosecond to millisecond time regime. For this and other reasons, myoglobin affords an ideal system for x-ray investigations.

To get an idea of the feasibility of using time-resolution x-ray spectroscopy to study molecular dynamics in biological systems, we decided to test our ability to follow the recombination of carbon monoxide and myoglobin after dissociation by a pulsed Nd:YAG laser, a process known to have a high quantum yield and to produce no photochemical reactions other than CO photodissociation. We chose to probe this recombination process by monitoring the near-edge structure in the x-ray absorption spectrum of the binding site atom, iron. One collects near-edge absorption data by measuring the absorption of the sample as a function of x-ray energy over an x-ray absorption edge of the atom of interest, in our case the K edge of iron.11 The energy position of the absorption edge is sensitive to the local environment of the absorbing atom, and one sees shifts of several electron volts as both the species and distribution of the atomic near-neighbors are altered. This effect is clearly visible in the static spectra of deoxymyoglobin and carboxymyoglobin (MbCO) shown in figure 6a. We used this energy shift to monitor the recombination of the carbon monoxide molecule with the iron atom after laser flash photolysis. Figure 6b gives the preliminary results. 12 Shown are four near-edge spectra resolved in time (colored lines), in each case in comparison with the spectrum of the recombined MbCO complex (black lines). The position of the deoxymyoglobin x-ray absorption edge in the first two spectra of figure 6b is clearly shifted towards lower energy relative to the MbCO spectrum, signifying that a substantial fraction of the carbon monoxide has not yet recombined with the myoglobin. The third spectrum of the figure gives the first indication of near-complete recombination. By the time of the fourth spectrum, the curves are by and large identical, indicating complete recombination.

While this experiment, with its time resolution of several hundred microseconds, did not make explicit use of the pulsed nature of the x-ray source, I have nonetheless described it here because it is a good example of the type of time-resolution spectroscopy experi-

Stroboscopic image of a Rayleigh wave traveling in a LiNbO<sub>3</sub> intermediate frequency television filter. The filter was driven at 37.46 MHz, the twelfth harmonic of the synchrotron-radiation source frequency. In this x-ray topograph of the (1321) reflection, the broad white line corresponds to a subgrain boundary.

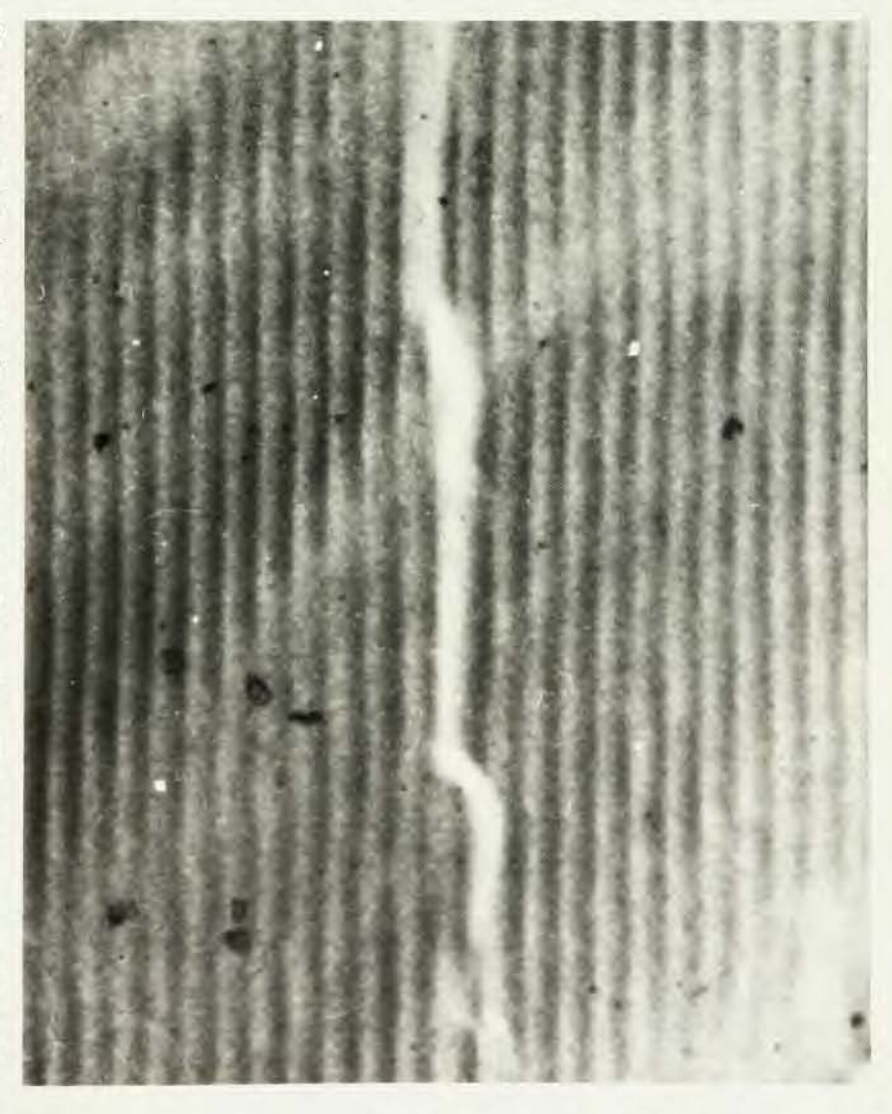
ments that one can perform. The initial results are quite encouraging, particularly in light of the fact that the data collection time was limited by the 20 Hz repetition rate of the Nd:YAG laser and not by the x-ray flux. Future plans call for increasing the time resolution to the sub-microsecond regime and looking into the possibility of collecting extended x-ray absorption fine structure (EXAFS) spectra,11 which should allow us to obtain detailed information, with a spatial resolution of better than 0.1 A, on the structural rearrangement that occurs around the iron-atom binding site.

Time-of-flight spectroscopy. When an atom absorbs a photon energetic enough to eject an inner-shell electron, that atom can de-excite through several channels, including fluorescent, Auger and Coster-Kronig transitions. The net effect of such transitions is to transfer the inner-shell vacancy to the outer shells. This is accomplished with no net change in the charge state of the atom in the case of radiative transitions, and with a net change in the

atom's charge state in the case of nonradiative transitions. The rapid rearrangement of electrons, known as a vacancy cascade, occurs on a time-scale of  $10^{-15}$  sec.

The significance of the vacancy cascade was pointed out experimentally in 1966, when physicists found<sup>13</sup> that after an L-shell vacancy was produced by photoabsorption in the iodine atom in CH3I, the ensuing vacancy cascade caused the molecule to decompose into its constituent atoms. Further work revealed that the electronic rearrangement accompaning the production of an inner-shell vacancy has a disintegrative effect on a number of compounds. Atomic processes such as this in isolated or small clusters of atoms are very interesting from a theoretical viewpoint. However, there have been few x-ray measurements of these processes because of the severe experimental difficulties involved-high temperatures, low pressures, low densities, and

Vaclav Kostroun of Cornell and Jerry Hastings of Brookhaven are continu-



ing one of these experiments, <sup>14</sup> using the tunable, pulsed x rays from CHESS, coupled with a time-of-flight spectrometer, to record the charge state of krypton atoms that they had excited with monochromatic x rays. The charged ions are first accelerated to give them the same kinetic energy per unit charge, and then allowed to drift toward a detector. The ions' arrival times at the detector then indicate their charges.

Figure 7a shows the ion spectrum when the incident x-ray energy is below the K-absorption edge of krypton; figure 7b shows the spectrum when the x-ray energy is above the edge. One can see that when the x rays are energetic enough to eject K electrons (figure 7b) the higher charge states (+8, +9 and +10) are much more intense, as would be expected because the photoejection of a K-shell electron opens another channel for the ejection of electrons through Auger deexcitation.

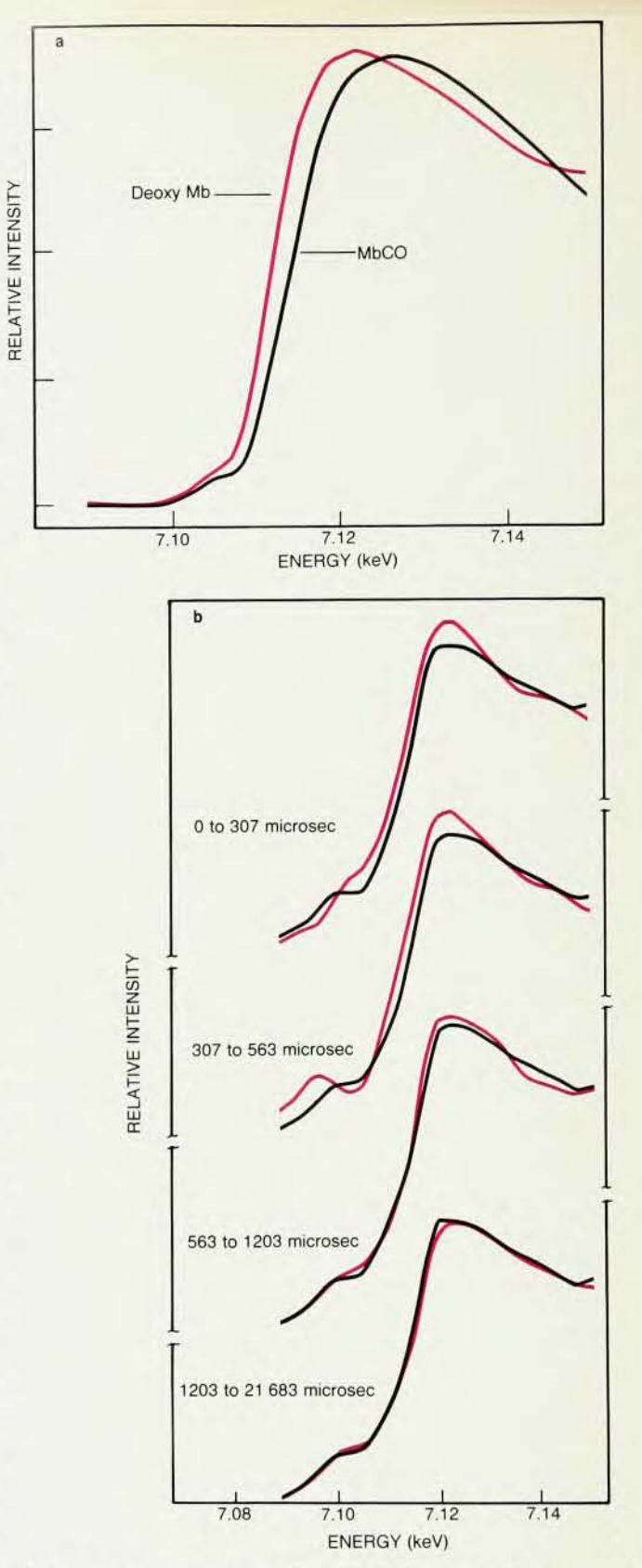
The extremely short (160 psec) x-ray pulses and long (2.56 microsec) interpulse periods at CHESS are ideally suited for time-of-flight experiments because there is little peak broadening from the nominal delta-function excitation pulse shape, and because the long periods between bursts reduces the temporal overlap of excitation and data collection.

Plans are now underway to expand these initial studies to include other elemental vapors and solid surfaces.

# **Future directions**

In the few examples described above we have seen how dynamical studies using diffraction, topography, spectroscopy and time-of-flight techniques have been performed in a wide range of scientific disciplines such as condensed-matter science, biochemistry, nuclear physics and atomic and molecular physics using pulsed x rays from storage rings. It should be straightforward to extend static studies into the regime of time resolution in other x-ray fields, such as Compton scattering, inelastic (thermal diffuse) scattering, crystallography and standing-wave studies.

Also, well-developed methods in other fields may be directly applicable to xray studies with time resolution. For example, the stroboscopic methods mentioned earlier are eminently suited to the high repetition rates available from storage-ring sources. By exciting the sample at some integral multiple of the repetition frequency of the emitted radiation, and systematically varying the relative phases between pump and probe, one can map the entire time evolution of the transient phenomena. Using stroboscopic techniques, one can acquire data with time resolution as quickly as one can collect the equivalent data on a static sample, and it is



Static and time-resolved x-ray absorption near-edge spectra of iron in deoxymyoglobin (Mb) and carboxymyoglobin (MbCO). Part a contains the static spectra, which show that the addition of the CO ligand causes a shift in position by about 3 eV of the iron edge relative to the deoxymyoglobin. Part b shows the spectra resolved in time (red lines) in comparison with the spectrum of the final time interval (dark line), at which the MbCO is fully recombined. The clear shift in the energy of the absorption edge seen in the first two spectra indicates a large fraction of the photolyzed CO has not yet recombined with the myoglobin. The numbers to the left of the curves show the time intervals (after the firing of the laser) during which the data were recorded.

not necessary to use high-speed detectors and data-acquisition systems to do so. We have already examined one exciting application of this method, namely stroboscopic topography. Equally promising is the prospect of expanding stroboscopic techniques to other diffraction experiments that will give detailed information on the dynamic behavior of a large class of systems operating at megahertz to gigahertz frequencies. Similarly, by synchronizing amplified mode-locked laser pulses to the frequency of the xray pulses, stroboscopic spectroscopies, including near-edge absorption spectra and exars studies should be feasible. This extension of stroboscopic techniques from crystalline samples to amorphous systems and solutions could enhance dramatically our knowledge of transient phenomena in biological, chemical and physical systems.

Frequency-domain or phase-shift methods<sup>15</sup> developed for fluorescence lifteime measurements with visible and ultraviolet synchrotron radiation are also applicable to x-ray studies that require time resolution. Calculations indicate that even with an incident burst several hundred picoseconds in duration, it may be possible to realize time resolution in the subpicosecond regime.<sup>15</sup> Such resolution, however, puts heavy demands on the stability of the storage-ring repetition frequency and on the consistency of the shape of the particle bunches.

Equipment development will play a crucial role in the future of time-resolution studies. New or improved designs of magnetic optics for accelerators could allow very short pulse durations during special runs dedicated to time studies. Designers of the next generation of storage rings are hoping to achieve pulse lengths of several picoseconds under special running conditions. Short pulses, however, would severely limit the maximum stored current and the beam lifetime.

User-adjustable repetition rates are certainly possible. One possibility is to allow the user to select the number of rf buckets to be filled during special timing runs. A more sophisticated scheme might give the user control of a fast vertical kicker that deflects one or several bunches out of the orbital plane in such a way that the experiment sees light only from the displaced bunches. In this manner the user could vary repetition rates from essentially 0 Hz to the natural repetition rate of the ring. Michael Hart of King's College in London suggests the use of x-ray optics to control the time structure at least of monochromatic radiation. He has considered various types of beam modulator monochromators, including rotating and vibrating crystals16 and x-ray interferometric devices17 that should

be capable of working at megahertz frequencies, so that every other, or every third x-ray pulse, for example, may be directed onto a sample.

As investigators try to collect more and more information in shorter times, they will surely require higher x-ray fluxes. The development of wigglers and undulators<sup>18</sup> will certainly help to relieve this problem. Particularly important will be the development of the x-ray undulator with a primary output peak wavelength of or below about 1.5 Å.

There is a need for better high-speed, gated, one- and two-dimensional detectors. Fast phosphors and scintillators with a high quantum efficiency for x-ray down-conversion will definitely be needed, along with the ability to record separately more than one photon per burst.

Many advances will come from parallel improvements on a number of fronts. For instance, wigglers and undulators and monochromators used in conjunction with high-speed, gateable, position-sensitive one-dimensional detectors may in the future allow one to collect entire time-resolved EXAFS or near-edge spectra with nanosecond resolution in only a few seconds.

Finally, what is most valuable is the imagination and ingenuity of the experimenters developing new techniques and bringing forth new systems to study. Synchrotron radiation has clearly shown itself to be an extremely versatile research tool, having already been applied to an impressive array of exciting problems in such diverse fields as engineering, medicine and the physical and biological sciences. We can look forward to seeing this list of problems expanded to include transient phenomena.

My thanks go out to the numerous colleagues I have contacted who have supplied me with information, data and figures for this article. I am especially appreciative of B. Batterman, P. Hartman, R. Siemann, J. Wilkens, D. Bilderback and S. Durbin for sharing their thoughts on this manuscript. I would also like to acknowledge the support of the National Science Foundation through grant number 81-12822.

### References

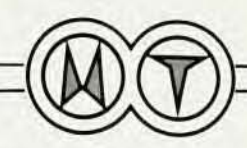
- See for example R. Lopez-Delgado, A. Tramer, I. H. Munro, Chem. Phys. 5, 72 (1974); K. M. Monahan, V. Rehn, Nucl. Inst. and Meth. 152, 225 (1978); N. Schwentner, U. Hahn, D. Einfeld, G. Muhlhaupt, Nucl. Inst. and Meth. 167, 499 (1979); I. H. Munro, N. Schwentner, Nucl. Inst. and Meth. 208, 819 (1983); I. H. Munro, A. P. Sabersky in Synchrotron Radiation Research, H. Winick, S. Doniach, eds., Plenum, New York (1980).
- For a detailed description of the operation of storage rings, see M. Sands in



# 2 kV : 2 mA POWER SUPPLY



Model 255 \$600.00

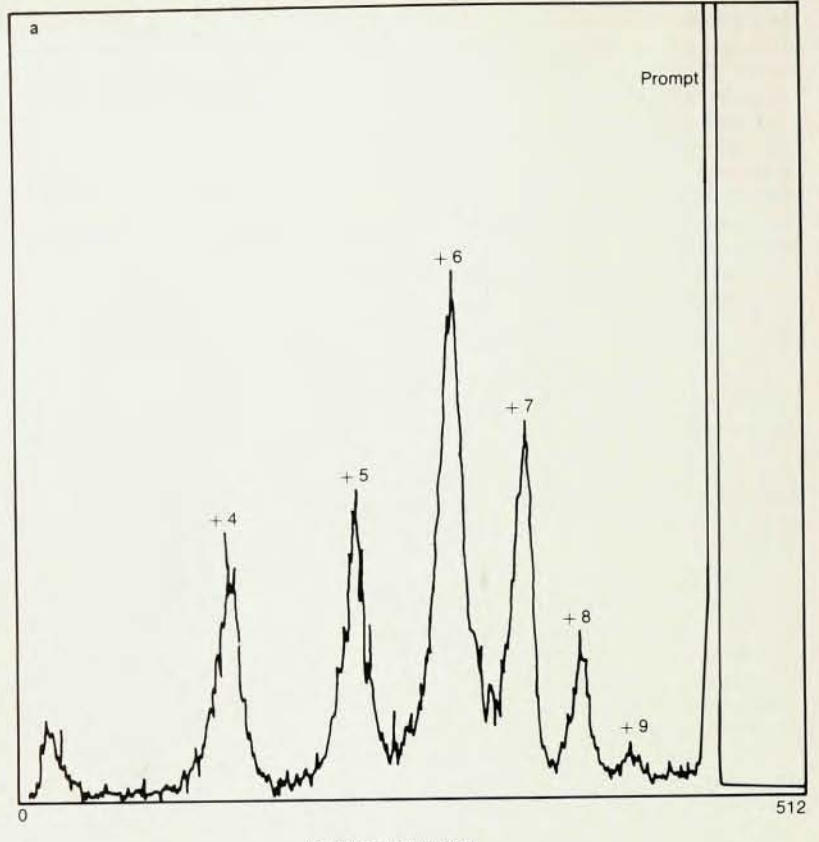


- Single Width NIM
- 0 to 2 k V Output with Front Panel Meter
- Reversible Polarity with Front Panel Indicators
- Output Short Circuit and Arc Protected

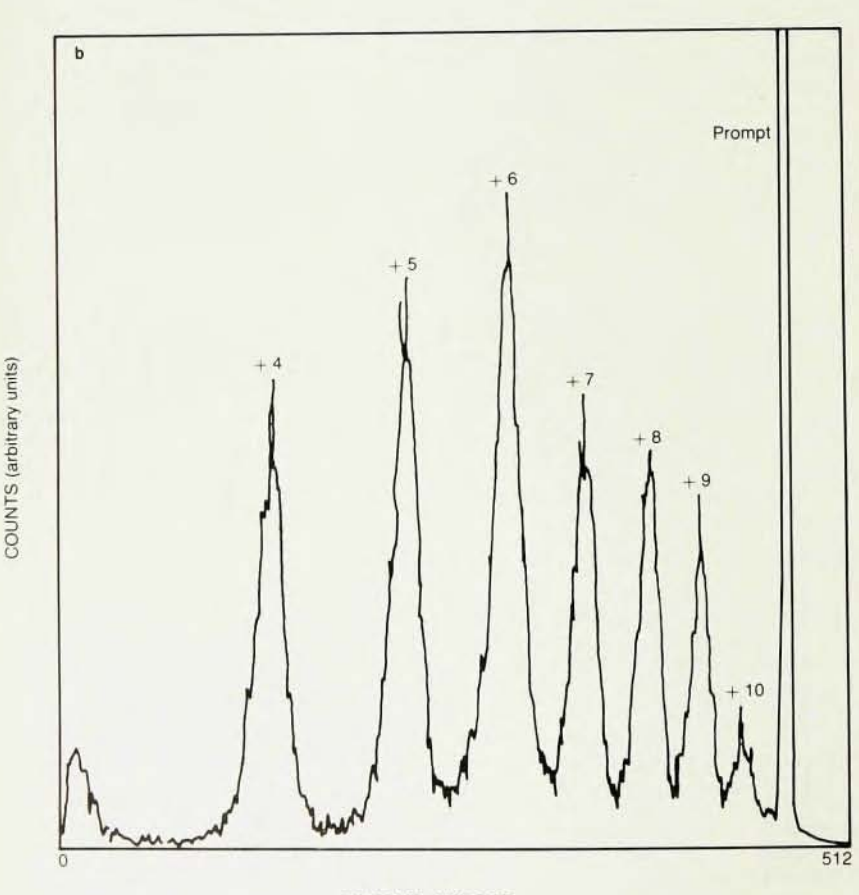
**Mech-Tronics** 

NUCLEAR

430A Kay Ave., Addison, II. 80101 For more information WRITE OR CALL COLLECT (312) 543-9304



CHANNEL NUMBER



CHANNEL NUMBER

Charge states following vacancy cascades in krypton, as measured with a time-of-flight spectrometer. a: Multichannel analyzer output when the incident x-ray energy is below the K absorption edge of krypton gas. b: Output when the incident x-ray energy is above the K edge. The vertical axis gives the number of ions detected, while the horizontal axis gives the arrival times of the ions. The charge assignments shown for the various peaks are tentative.

Proceedings of the International School of Physics—Enrico Fermi, B. Touschek, ed., Academic, New York (1971), page 257.

- C. Benard, M. Rousseau, J. Opt. Soc. Am. 64, 1433 (1974); R. Lopez-Delgado, Opt. Comm. 27, 195 (1978).
- R. L. Cohen, G. L. Miller, K. W. West, Phys. Rev. Letts. 41, 381 (1978).
- J. C. Wang, R. F. Wood, P. O. Pronko, Appl. Phys. Lett. 35, 455 (1978); R. F. Wood, G. E. Giles, Phys. Rev. B 23, 2923 (1981).
- V. Heine, J. A. Van Vechten, Phys. Rev. B 13, 1622 (1976); J. A. Van Vechten, R. Tsu, F. W. Saris, D. Hoonhout, Phys. Lett. 74A, 417 (1979); J. A. Van Vechten, M. Wautelet, Phys. Rev. B 23, 5543 (1981).
- B. C. Larson, C. W. White, T. S. Noggle,
   D. M. Mills, Phys. Rev. Lett. 48, 337 (1982);
   B. C. Larson, C. W. White, T. S. Noggle, J. F. Barhorst, D. M. Mills, Appl. Phys. Lett. 42, 282 (1983).
- C.-C. Glüer, W. Graeff, H. Moller, Nucl. Inst. and Meth. 208, 701 (1983).
- P. A. Goddard, G. F. Clark, B. K. Tanner, R. W. Whatmore, Nucl. Inst. and Meth. 208, 705 (1983); R. W. Whatmore, P. A. Goddard, B. K. Tanner, G. F. Clar, Nature 299, 44 (1982).
- P. G. Debrunner, H. Frauenfelder, Ann. Rev. of Phys. Chem. 33, 283 (1982); J. A. McCammon, M. Karplus, Acc. Chem. Res. 16, 187 (1983).
- For a more detailed account of x-ray absorption spectroscopic techniques, see H. Winick, S. Doniach, eds., Synchrotron Radiation Research, Plenum, New York (1980).
- D. M. Mills, A. Lewis, A. Harootunian, J. Huang, B. Smith, Science 223, 811 (1984).
- T. A. Carlson, R. M. White, J. Chem. Phys. 44, 4510 (1966).
- J. B. Hastings, V. O. Kostroun, Nucl. Inst. and Meth. 208, 815 (1983).
- V. Rehn, Nucl. Inst. and Meth. 177, 193 (1980); E. Gratton, R. Lopez-Delgado, Rev. Sci. Inst. 50, 789 (1979).
- M. Hart in Characterization of Crystal Growth Defects by X-Ray Methods, B. K. Tanner, D. K. Bowen, eds., Plenum, New York (1980), page 479.
- M. Hart, D. P. Siddons, Nature 275, 45 (1978).
- 18. For a description of wigglers and undulators for enhanced x-ray flux, see H. Winick, G. Brown, K. Halbach, J. Harris, PHYSICS TODAY, May 1981, page 50; G. Brown, K. Halbach, J. Harris, H. Winick, Nucl. Inst. and Meth. 208, 65 (1983).